

國立臺灣大學生命科學院生命科學系碩士論文
Department of Life Science, Institute of Life Science
National Taiwan University



表現視黑質之視神經細胞
藉視網膜內之軸突分支接觸無軸突細胞
Melanopsin Expressing Retinal Ganglion Cells
Connect to Amacrine Cells
By Intra-retinal Axon Collateral

研究生：葉柏廷

Advisee：Yeh, Po-Ting

指導老師：陳示國 助理教授

Advisor: Dr. Chen, Shih-Kuo

中華民國 104 年 2 月

February, 2014

致謝



這本論文的完成與碩士班的路途中，得到來自許多人的幫助，難以一一列出，我只能在這裡精簡的列出希望特別感謝的人們。

首先我要感謝我的指導教授陳示國老師，在剛回到台灣，實驗室尚未建立時，便願意接納沒有太多神經生物學基礎的我，並且最簡單的實驗開始帶我做起，一直到一步一步完成這份論文。除了學術上的指導之外，老師也以學長和夥伴的身分和我分享許多生活經驗與歷程，讓我獲益許多並且增添了實驗室的愉快回憶。

在生命科學館六年半以來，我想特別感謝我的大學導師，同時也是口試委員之一的潘建源老師。從大學生活、研究所指導老師選擇以至於碩士班口試，都給了我許多相當有建設性的建議。

我想感謝實驗室的夥伴們。你們給我許多工作與情感上的支持，包容了我能力不足的地方，也讓我在台北有個像家一般溫馨的地方！來自朋友們的鼓勵、脂肪和酒精讓我度過許多難關，我忘不了在麻將桌上討論各自實驗的場景。相識多年，身兼同學、同事和室友的王惠民往往在我分身乏術時給予及時的幫助，實驗買菜調酒甚至弄了前所未見的口視轉播，包山包海不一而足，是我最忠實的夥伴。

碩一認識進而交往的女友愛鵬，用滿滿的愛支持著我。我們一起哭、一起笑，一起牽著手走過這一段路。妳總是給我許多意想不到的驚喜，陪我完成許多願望。謝謝妳願意很有耐心地提醒我許多，並願意等待我在過程中，變得成熟與懂事一些些。

最後我想感謝我的父母與家人，還有來不及看到這句話的阿公。你們成就了今天的我，也期望你們會對這一刻感到一絲絲的驕傲。

中文摘要



視網膜的結構與神經迴路已經被研究了一百多年。傳統認知中訊號如此傳遞：視桿細胞與視椎細胞接收光訊號並且轉換為神經衝動，將訊號傳遞至水平細胞、無軸突細胞與雙極細胞，並且藉由視神經細胞傳遞到腦。近期研究指出除了上述的路徑之外，一類視神經細胞，即自主感光視神經細胞，能夠藉由未知的方式傳遞回饋訊號至上游部分種類的無軸突細胞。其他研究也指出自主感光視神經細胞具有視網膜內的軸突分支，深入是網膜中的內網狀層，然而這些軸突分支的型態與功能等都尚未被發掘。藉由基因轉殖與隨機標定小鼠視網膜上的自主感光視神經細胞，我們發現兩組型態各異的軸突分枝；此外我們也發現這些軸突分枝會與多巴胺無軸突細胞產生神經連結。我們的實驗結果支持自主感光神經細胞能夠藉由軸突分枝將訊號傳給無軸突細胞，並且可能藉此進一步影響視網膜的功能。

關鍵字：自主感光視神經細胞、無軸突細胞、軸突分支、視網膜迴路

ABSTRACT



Retinal structure and functional circuits have been studied for more than a century. It is well known that the information flow of retinal circuit starts from light reception by rods and cones, to horizontal cells, amacrine cells and bipolar cells, and transduces to brain by retinal ganglion cells. However, recent studies indicated that a group of melanopsin containing retinal ganglion cells, named intrinsically photosensitive retinal ganglion cells (ipRGCs), send feedback signals to a specific sub-population of amacrine cells by an unknown mechanism. Recent studies showed that ipRGCs contain intra-retinal axon collaterals that stratified in the inner plexiform layer, yet the morphology and functions of these collaterals remain unclear. By randomly genetically labeling of ipRGCs in mice, our study shows two morphologically distinct types of ipRGC intra-retinal axon collaterals. We also found those collaterals connect to dopaminergic amacrine cells. Our finding suggests that ipRGCs send feedback signals to amacrine cells via intra-retinal collaterals, which may modulate retinal functions.

Content



口試委員審訂書	i
致謝	ii
中文摘要	iii
Abstract	iv
Content	v
Figure content	vii
Chapter 1. Introduction	1
1.1 Conventional knowledge to retinal circuitry.....	1
1.2 Intrinsically photosensitive retinal ganglion cells.....	3
1.3 Intra-retinal feedback signals from ganglion cells.....	7
1.4 Intra-retinal axon collaterals of retinal ganglion cells.....	9
Chapter 2. Material and methods	11
2.1 Animals	11
2.2 Retina harvesting	12
2.3 NBT/BCIP staining and whole mount imaging	12
2.4 Frozen cross section	13
2.5 Triple staining and confocal imaging	14
2.6 Electroporation retina culture	15

2.7 Transmission electron microscopy	16
Chapter 3. Results	19
3.1 Morphology of ipRGCs with intra-retinal collaterals	19
3.2 Connection of ipRGCs intra-retinal collaterals and amacrine cells	21
3.3 IpRGCs express synaptophysin in cultured retina	24
3.4 Ultrastructure of ipRGCs intra-retinal collaterals	25
Chapter 4. Discussions	26
4.1 Significance of the work.....	32
Figures	33
References	48
Appendixes	56
Buffers and formulas	56
Chemicals and commercial reagents	62
Devices	63

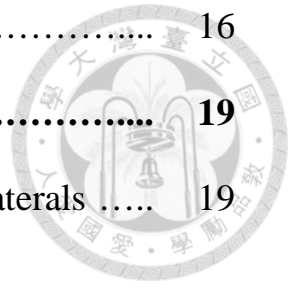


Figure content



Figure 1 Hypothesis.	33
Figure 2 Morphological characteristics of intrinsically photosensitive retinal ganglion cells intra-retinal axon collaterals.	34
Figure 3 Collateral of ipRGCs contact with to dopaminergic amacrine cells.	37
Figure 4 Cross section view of an ipRGC collateral.	39
Figure 5 Collateral of ipRGC connect to DAC neurites.....	41
Figure 6 Melanopsin positive RGCs in cultured retina express synaptophysin.	43
Figure 7 Synaptic ultra-structure of ipRGC collateral.	45
Figure 8 Illustration of the conclusion.	47

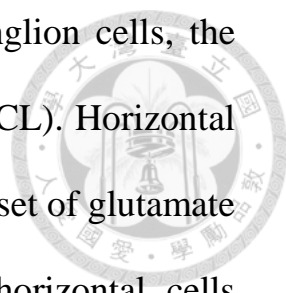
Chapter 1. Introduction



1.1 Conventional knowledge to retinal circuitry

Retina and retinal circuits have been studied for more than a century. Retina, composed with high density of neurons, is a thin tissue located at the back of an eye and is essential for mammalian visual functions. In a retina, different types of neurons are arranged into three distinct layers. The outermost layer is the photoreceptor layer filled with rod cells and cone cells. These conventional photoreceptors contain photopigments rhodopsins or cone type opsins which convert light to neural activities. Once absorbing energy from light, retinol conjugated with opsins transforms from *11-cis* form to *all trans* form, which activates opsin coupled G protein. G-protein activates cGMP phosphodiesterase, which decreases cell cGMP concentration by hydrolyzing cGMPs. Low cGMP level closes sodium channels on photoreceptors, making photoreceptors no longer depolarized. Unlike most neurons, photoreceptors hyperpolarize to encode signals from light.[1, 2]

The second layer is inner nucleus layer (INL) consisted with three different type of interneurons including horizontal cells, bipolar cells and amacrine cells. Bipolar cells receive light information from photoreceptors through synaptic input in the outer plexiform layer (OPL).



The bipolar cells then transmit the signal to retinal ganglion cells, the innermost neurons in the retina, at ganglion cell layer (GCL). Horizontal cells receive signals from photoreceptors by expressing a set of glutamate receptors in OPL as well as bipolar cells. While horizontal cells processes to form synapse at OPL, amacrine cells form synaptic connections with other retinal neurons at inner plexiform layer (IPL). Horizontal cells and amacrine cells provide lateral computations and adjust retinal function such as light/dark adaptation and modulation of receptive-field. The output signals of amacrine cells also send to other cell layers as bipolar cells do, response for ca. 30% of inner nucleus layer output to ganglion cells.[3]

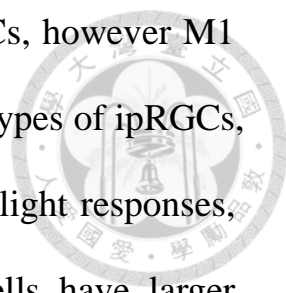
The responses of retinal ganglion cells are more complex processing systems than photoreceptors and other interneurons. By comparing signals from their “on” and “off” reception fields, different types of retinal ganglion cells can response to color opponency, edge detection and moving objects in their receptor fields. At the same time, axon of retinal ganglion cells converge to optic disc in center retina, project to lateral geniculate nucleus through the optic nerve, optic tract and present final conclusions from retina.[3]

1.2 Intrinsically photosensitive retinal ganglion cells

A novel mammalian photoreceptor expressing melanopsin was discovered by immunohistochemistry.[4, 5] Melanopsin was first cloned from the skin of *Xenopus laevis*, or African clawed toad, a frog species commonly used as experimental model.[6] Like rhodopsin and cone opsins, melanopsin, or opsin 4 (gene name *Opn4*) is one type of light sensitive photopigment. Interestingly, melanopsin-expressing neurons were found in mammalian retina as well including rodents, cats, monkeys and human.[4, 5, 7] However, this novel opsin is not expressed by rods and cones, but surprisingly expressed by a sub population of retinal ganglion cells (RGCs).[5, 7, 8]

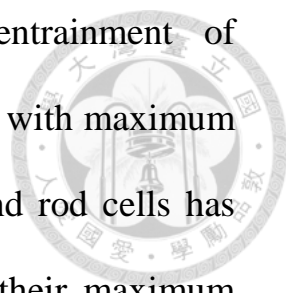
These melanopsin-expressing cells not only receive light signals from bipolar cells and amacrine cells as regular RGCs, but are light sensitive by themselves, hence named intrinsically photosensitive retinal ganglion cells (ipRGCs).[5, 7, 8] Compared to conventional photoreceptors, intrinsically light responses of ipRGCs are delayed and sustained. Intrinsically photosensitive retinal ganglion cells are currently classified into five subtypes, named M1~M5. Subtypes of ipRGCs are different in several ways including stratification patterns in IPL, dendritic fields, soma sizes and several electrophysiological characters.[9, 10]

Dendrites of M1 cells stratify in “off” division of the IPL where



off-bipolar cells form synaptic connections with off-RGCs, however M1 cells receive signals mostly from on-bipolar cells. Of all types of ipRGCs, M1 cells exhibit highest and most sensitive intrinsically light responses, however light responses from cones are small. M2 cells have larger dendritic field and stratify in “on” IPL and also have larger soma size. In contrast to M1 cells, M2 cells have small intrinsically light responses but large responses to inputs from cone cells. Stratification patterns of M3 cells are special by its bistratification in both “on” and “off” IPL. Otherwise, M3 cells have similar dendritic field, soma size and electrophysiological response to M2 cells. M4 cells have largest soma sizes and dendritic fields, which stratify at “on” IPL.[9] The intrinsically photosensitivity of M4 cells are lower threshold, while other physiological properties of M4 cells remains unknown. A study suggested conventional on α RGCs are intrinsically photosensitive and they may be M4 ipRGCs.[9, 11] Mice lacking either melanopsin or ON alpha RGCs have behavioral deficits in contrast sensitivity. These findings indicate a role for melanopsin and ipRGCs in vision.[9] The last one, M5 cells have small and highly branched dendrites stratified in “on” IPL. Other than cell morphology, we don’t know much about M5 cells.[9]

Intrinsically photosensitive retinal ganglion cells are found to relate to different non-visual light functions, including long studied circadian

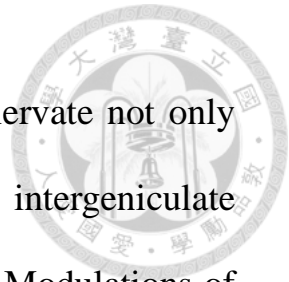


photoentrainment and pupil light reflex.[12] Photoentrainment of mammalian circadian clock is mediated by photoreceptor with maximum absorption at ca. 480 nm wavelength.[13] Rhodopsin and rod cells has been as likely candidates for photoentrainment due to their maximum absorption wavelength, however their absorption spectrum does not fit the results of phase shift experiments.[13] Moreover, studies showed that even on conventional photoreceptor elimination mice, the circadian photoentrainment remains.[14] All these evidences suggest that circadian photoentrainment is mediated by a non-rod novo photoreceptor with maximum absorption similar to rhodopsin and rod cells. Intrinsically photosensitive retinal ganglion cells innervating suprachiasmatic nucleus (SCN) are proven to be such novo photoreceptor after its discovery.[12, 15]

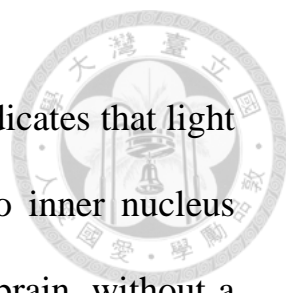
Pupil light reflex (PLR) as well as in other non-image-forming visual function, has been studied for a long time. Studies showed PLR remains on rod and cone cell elimination mice but reduced on melanopsin knocked out mice.[16] The nucleus control PLR in the brain, the olivary pretectal nucleus (OPN), are innervated by ipRGCs, indicating melanopsin expressing ipRGCs send light signal directly to OPN, and by this mean control PLR.[16-18] Besides retina-OPN pathway, a recent study showed that a group of melanopsin positive cells in ciliary marginal

zone are also responded for PLR.[19]

Intrinsically photosensitive retinal ganglion cells innervate not only SCN and OPN, but also longitudinal geniculate nucleus, intergeniculate leaflet, superior colliculus and other regions in the brain. Modulations of ipRGCs to these brain regions are largely unknown. On the other hand, ipRGCs are possibly related to migraine photophobia, season affective disorders and other physiological functions, by known means. [6, 8, 9, 18]



1.3 Intra-retinal feedback signals from ganglion cells

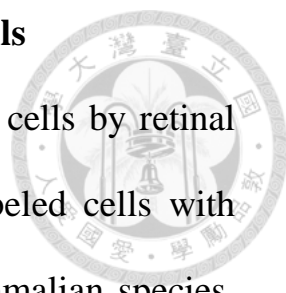


Although conventional concept of retinal circuitry indicates that light signal flow in retina is unipolar, from photoreceptors to inner nucleus layer then to retinal ganglion cells and finally output to brain, without a backward feedback pathway from RGCs. Recent electrophysiology research showed that ipRGCs can influence the firing rate of dopaminergic amacrine cells (DACs), the only neurons that release dopamine in the retina, through unknown way.[20-22] The concentration of dopamine in the retina is controlled by direct light input and also circadian rhythm.[23-27] The level of dopamine increases during the subjective day and decreases during the subjective night.[27] This daily oscillation of dopamine level, which controls a broad range of temporal retinal physiology including visual photopigments expression and visual processing, is independent of mammalian master biological clock suprachiasmatic nucleus.[26] Dopamine regulates retina acutely by modulating the gap junction permeability between photoreceptor and retinal ganglion cells under light adaptation.[23-25, 28] Therefore, the regulation of dopamine release from DACs plays an important role on retinal light detection functions.

Another evidence also indicates that light input through ipRGCs can modulate the retinal ganglion cell afferents segregation structures in the

lateral geniculate nucleus without innervate them.[29] Furthermore, ipRGCs can also modulate cholinergic retinal wave regulated by starburst amacrine cells during retinal development. How ipRGCs send feedback signals to amacrine cells is not clear until now.[29] Several hypothesis are raised to explain the possible mechanism for ipRGCs to send feedback signal to DACs. Signals can be sent from neurons by axonal-dendritic synapses, diffused neurocrine molecules, or atypical dendritic-dendritic synapses. Since the light signal from ipRGC can trigger the action potentials firing on DACs even without rod and cone input, it is unlikely that ipRGCs use neurocrine to send feedback information to DACs.[21, 22] Therefore, axonal-dendritic or dendritic-dendritic synapses are more convincing pathways for ipRGC to communicate with DACs.

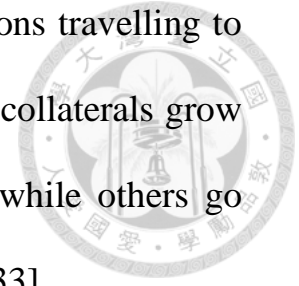
1.4 Intra-retinal axon collaterals of retinal ganglion cells



Intra-retinal collaterals are found on retina ganglion cells by retinal dye injection in single RGC. About 1% of random labeled cells with intra-retinal branches were observed from multiple mammalian species, including cat, turtle, rabbit, monkey, human and rodents.[30-32] The collaterals were first found on cat retina by extracellular, iontophoretic injections of horseradish peroxidase.[32] The collaterals are morphologically distinct from ganglion and amacrine cell dendrites, extend widely and terminate within the inner plexiform layer.[31, 32] The collaterals are long and straight, approximately 1 μm in diameter, and in some cases can be traced for several millimeters in the inner plexiform layer. Terminal branches of these collaterals are widely spaced so that the bouton clusters are distributed in small, isolated patches along the length of the collaterals.[32] Bouton clusters vary in size and single boutons are frequently large, up to 3 μm in diameter.[32] Boutons on the collaterals of RGCs indicate RGCs may send signals back to outer retina via these intra-retinal axonal branches.

Further study of our lab showed some ipRGCs, mostly in M1 subtype, have intra-retinal collaterals as well.[33] By titrated tamoxifen injection on $\text{Opn4}^{\text{CETL}}$ and $\text{Rosa26}^{\text{HPAP}}$ mice, ipRGCs are sparsely labelled, thus intra-retinal collaterals of ipRGCs were revealed. The

collaterals are varied in size, branch point from main axons travelling to thalamus, axonal fields and stratification patterns. These collaterals grow back to IPL, some of them stratify in “on” sub-layer, while others go further to “off” sub-layer, both with unknown functions.[33]



Chapter 2. Material and methods



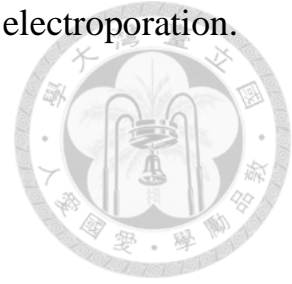
2.1 Animals

Transgenic B6/129 mice raised under 25°C, RH 50%, 12:12 hr light dark condition were used in experiment. To identify ipRGCs, we used transgenic B6/129 mice and Cre-Lox recombination system. Two transgenic lines were employed. $Opn4^{CETL}$ line stands for $cre^{ER/T2}$ knocked in to melanopsin locus, promote by $Opn4$. $Cre^{ER/T2}$ is a recombinase modified from cre and its permeability to nucleus is controlled by applied tamoxifen dose. Once $cre^{ER/T2}$ permit into cell nucleus, it recombine gene inserted with loxP.[34-36] $Rosa26^{HPAP}$ stands for knocked in human placental alkaline phosphatase, can be activated by cre and promoted by universal promotor Rosa26. Alkaline phosphatase transfer chromogen NBT/BCIT into purple-blueish precipitation, which is visible under bright field microscope, confocal microscope in reflex mode. The precipitation is also electron dense and detectable under transmission electron microscopy (TEM).[37]

We crossed $Opn4^{CETL}$ and $Rosa26^{HPAP}$ line. By applying low dose of tamoxifen (0.2-0.3 mg on each animal by intrapleural injection, at least 10 days before harvesting), we could sparsely label ipRGCs on adult mice. (Figure 2A) Another line $Opn4^{cre}$ with unmodified cre was also

employed to selectively express external vectors sent via electroporation.

(Figure 6A)



2.2 Retina harvesting

Adult animals pretreated by tamoxifen were anesthetized by over dose avertin (0.5 mg avertin per gram). Fully anesthetized animals were perfused with 7.5 mL of phosphate buffer saline, pH 7.4 (PBS) on ice and then 45 mL of 4% paraformaldehyde solved in phosphate buffer, pH 7.4 (PFA/PB) on ice in 3mL/min rate by perfusion pump. Eye balls were carefully harvested. Eyes were post-fixed in room temperature 4% PFA/PB for 30 min then wash in PBS. Eyes were dissected in PBS and cornea, lens and sclera respectively were carefully removed, remained the retinae. We made four radial release cut on extracted retinae to ease follow flattening procedure. (As shown in Figure 3A, Figure 6A and Figure 7A) Retinae were processed immediately depends on observation requirement.

2.3 NBT/BCIP staining and whole mount imaging

Extracted retinae were flattened and fixed in 4% PFA/PB between glass slide and parafilm at room temperature, 4 hr. Retinae were washed 3 times by PBS in room temperature, each for 30 min. (This preparation

is only required for retinae needed for further immunohistochemistry.) We heated retinae in 60°C PBS for 45 min to inactivate endogenous alkaline phosphatase. Heat stable HPAP would remain activity. We applied NBT/BCIP solution (1/4 tab solved in 2.5 mL ddH₂O) for 12 to 16 hr in room temperature, avoided light. Retinae were washed 3 times by PBS, room temperature, each for 10 min. We mounted retinae in 50% glycerol and 50% PBS for observation.

Whole-mounted retina images were taken under brightfield microscope. NBT/BCIP positive neurons with intra-retinal collateral were recorded under differential interference contrast (DIC) imaging in serial focal plans to observe stratification pattern of collaterals in inner plexiform layer.

2.4 Frozen cross section

Glycerol mounted retina sample were rinsed in PBS for several times. Samples were immersed into 30% Sucrose for 1hr and then immersed commercial “*optimal cutting temperature (OCT)*” embedding compound for another 1hr. Retinae were mounted in OCT between 2 coverslips, which flattened retina by surface tension. The coverslip sets were frozen on sample preparing stage in cryostat microtome. We removed one coverslip by razor and added extra OCT compound on the exposed retina

face, and repeated above procedure on the other side of retina to embed entire flattened retina. Retinae set onto specimen arm of the microtome were cut by cross section direction, perpendicular to cell layers in particular, in 20 μ m thickness. Sections were attached on glass slides with positive charge. We placed section carrying slides into electronic dry cabinet (RH<30%) immediately and dried for an overnight. Dried sample slides were ready for immunohistochemistry procedures. The slides were be stored in -20°C refrigerator if they were not used immediately after dried. Sections on slides were rehydrated by rinsing whole slide in PBS for 5-10 min for further procedures.

2.5 Triple staining and confocal imaging

We applied blocking solution to extracted retinae or rehydrated retina sections attached on glass slides for 6 hr, room temperature. Then we applied new blocking solution with antibodies (concentration described in “buffers and formulas” in appendix) for an overnight, 4°C. Samples were washed 3 times in room temperature PBS, each for 1 hr. We applied blocking solution with secondary fluorescent antibodies (concentration described in “buffers and formulas” in appendix) for 2 hr in room temperature. Samples were washed 3 times by room temperature PBS, each for 30 min. Retina samples were mounted with *Vectashield with*

DAPI for observation.

For sections on glass slides, blocking solutions with or without antibodies were gently added on the slides by 200 μ L. We covered the slides with parafilm and put it into moist chamber to avoid drying. After gently removing parafilm, blocking solutions were removed by standing the slides on clean tissue paper to absorb liquid. For washing sections on slides, we immersed glass slides into a tank filled with PBS on shaker. After mounting, sections were firstly observed under light field microscope and compared with images in whole-mounted view to re-localize neurite puncta on sections to original retinae.

Confocal images were taken via 40x oil immersion lens and Zeiss Zen 2010 software.

2.6 Electroporation retina culture

Opn4^{Cre} line mice pups in postnatal day 2 were used for electroporation. Pups were anesthetized by isoflurane. We extracted retinae in dissecting buffer and attached each retina to a piece of sterilize filter paper. Filter papers and retina were immersed in to 300 μ L dissecting buffer contains 76 ng/ μ L plasmid for 10 min. This N1 vector carried loxP – dsRed – loxP - synaptophysin::eGFP (sequence was written in “buffers and formulas” in appendix), which

synaptophysin::eGFP could be activated in exist of cre and sent to axon terminal. Parameters of electroporation were 30 volt, 50 ms duration, and two shocks with 1 sec interval. After electroporation, retinae with filter paper were placed into culture medium, with 37°C and 5% CO₂ environment for five days. Culture medium were changed every day. After five days, retina samples were fixed in 4% PFA/PB for 20 min and mounted in glycerol for observation.

2.7 Transmission electron microscopy

Extracted retinae were flattened on glass slides and fixed in fresh-mixed 2% glutaraldehyde and 2.5% formaldehyde solved cacodylate buffer with sucrose (CBS) and covered by parafilm for 2 hr, then transferred into eppendorf and fixed for another 15 hr, both in 4°C. Retinae were washed three times in CBS, each for 10 min. We applied NBT/BCIP (1/4 tab solved in 2.5 mL ddH₂O) solution to retinae for 12-16 hr. Retinae were washed again in CBS and then mounted in 50% glycerol and 50% CBS to search NBT/BCIP positive neurite with collaterals co-stratified with DACs in IPL under brightfield microscope.

Glycerol mounted retina samples were rinsed in CBS for several times. We post fixed retinae by 1% osmium tetroxide solved with 0.1M cacodylate buffer for 10 hr, 4°C. Samples were washed three times in

CBS then another three times in distilled water. We dehydrate retinae in serial ethanol stages (30%, 50%, 75%, 85%, 95, 100% and 100% again). Samples were immersed into 3:1 of ethanol anhydrous and Spurr's resin A (described in buffer and solution formula), then 1:1, 1:3 and full Spurr's resin A, each for 8 hr, shaking in 4°C. We immersed retinae in Spurr's resin B four times, each for 8 hr, shaking in 4°C. Retinae with proper amount of Spurr's resin B were transferred into silicone mold, and hardened the resin in 60°C oven for 48 hr.

Cured resin blocks were trimmed to expose axon collaterals under dissecting microscope by razor. Trimmed surfaces were perpendicular to the collaterals while length of trimmed surfaces were shorter than 0.5 mm. Retinae were cut in cross section direction with ultramicrotome equipped fresh made glass knives. For each section set, 5-10 pieces of 90 nm ultra-thin section were cut and collected, then immediately cut a 0.99 μm semi-thin section, in order to compare brightfield semi-thin images and TEM ultra-thin images side by side. Semi-thin sections were collected on glass slides, counter stained by 1% safranin O solved in 50% ethanol for 90-120 sec, ca. 45°C. After dried thoroughly, glass slides were mounted with glycerol. After mounting, sections were observed under brightfield microscope and compared with images in whole-mounted view to re-localize neurite puncta on sections to original retinae. Ultra-thin

sections were collected on 50 mesh copper grids covered with formavor membrane (made of 0.5% solution, ca. 20 nm thickness).

We dried grids in electronic dry cabinet for at least an overnight. Samples on grids were stained by 2% uranium acetate for 20 min. We rinsed grids for 10-15 times in distilled water, repeated for 6 times. After staining, grids were dried in electronic dry cabinet for at least an overnight and then be ready for TEM imaging. TEM images were taken with 75 kV accelerating voltage, 40,000x to 70,000x magnification, with auto gain and exposure. [38, 39]

Chapter 3. Results



Recent evidence suggest that intrinsically photosensitive retinal ganglion cells could provide feedback information to other retinal neurons. We hypothesize that ipRGC intra-retinal collaterals co-stratified with dopaminergic amacrine cells are the means that ipRGCs send feedback signals to DACs.

3.1 Morphology of ipRGCs with intra-retinal collaterals

There are at least 5 types of ipRGC expressing melanopsin that covered the whole retina with extensive overlapping. Therefore, we combined Opn4 driven inducible Cre^{ER/T2} line with alkaline phosphatase reporter mouse line to reduce the number of labeled cell in order to reduce the ambiguity when multiple neurites from different cells occupying the same area. This method increased the spatial resolution and allowed us to analysis fine neurite architecture at single cell level. (Figure 2A) Due to principle of this methods, most ipRGCs we observed were off sublayer-stratified M1 cells, which express more melanopsin as well as knocked-in HPAP than other ipRGCs. In small percentage of M1 ipRGC, we observed axon collaterals branched out from the main axon that goes toward the optic disc. Some collaterals showed single

intra-retinal axon terminal while others showed multiple branches on collaterals. Moreover, terminals of 8 out of 17 observed collaterals reached deeply into S1 sublayer, while remain collaterals only reached shallower position in inner plexiform layer. (Figure 2B-F)

We further analyzed these two classes of collaterals. By measuring the distance between ipRGC soma and the branch point of the collateral axon, defined as branch distance, (Figure 2G) axon collaterals co-stratified with DACs showed significantly shorter branch distance compared to those reached shallower position in the IPL (student t test, $p=0.006$). This result suggests that there are at least two distinct populations of ipRGC form axon collaterals targeting different cell types in the retina. (Figure 2H)

3.2 Connection of ipRGCs intra-retinal collaterals and amacrine cells

To determine whether axon collaterals from ipRGC co-stratified with dopaminergic amacrine cells (DACs) at S1 sub-layer of the IPL connect to DACs, we performed multiple immunofluorescence staining and tried to observe co-localization of ipRGC collaterals, DACs and synaptic markers with help of confocal microscopy.

With no efficient antibodies to detect human placental alkaline phosphatase (HPAP) expressed by sparsely labelled ipRGCs, we used reflex mode of confocal microscope to detect NBT/BCIP precipitation. Tyrosine hydroxylase (TH) antibody was used as marker of dopaminergic cell. Due to specially non-polar character of amacrine cells, dendrites can be identify by anti-TH though the antibody bind on soma and axon only on typical dopaminergic cells. Finally bassoon antibody was used to detect synapse. Collaterals stratified S1 sublayer were searched under brightfield microscope (Figure 3A-C). We then took high magnified confocal images of those collaterals (Figure 3D-F). We observed several co-localization of HPAP, TH and bassoon. (Figure 3E-G, indicated by white arrows). However thickness of IPL (ca. 40 μm) reduced image quality.

To enhance spatial resolution power and permeability of antibodies, we employed frozen cross section to have thinner 20 μm tissue samples.

Cross section procedure of retinae improved another problem at the same time, which NBT/BCIP precipitation sheltered deeper tissue from confocal laser bin, substantially weakened signals of deeper tissue. We adjusted tilting of cross section plans and cut ipRGC collaterals vertically, hence minimized area sheltered by NBT/BCIP precipitations.

Collaterals stratified S1 sublayer were firstly search under brightfield microscope and whole-mount view as well. (Figure 4A-E) Figure 4B-E present DIC images of different focal plan from ganglion cell layer to boundary of IPL and inner nucleus layer, respectively. Cellular motifs in E indicate boundary of inner nucleus layer. We collected sections of axon terminals on collaterals (Figure 4F) and took confocal images (Figure 4G).

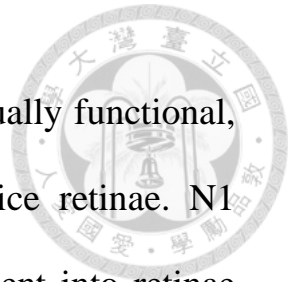
We applied different synaptic marker on the cross sections. Synaptophysin (SYP) and postsynapse dense (PSD) antibodies were applied to detect presynapse and post synapse, respectively. In higher magnification of Figure 4G, we found HPAP co-localized with SYP (Figure 5B, D-E) and TH co-localized with PSD (Figure 5C, F-G), and the two site connected together (Figure 5A). These images suggest ipRGC-to-DAC synapse are formed on ipRGC intra-retinal collaterals co-stratified with DACs. Other examples were shown in H-J. In our observation, postsynaptic dopamine neurites were diverse in diameter,

indicates both axon-like and dendrite-like DAC neurites are involve in the ipRGC-DAC feedback circuitry, which suggest different ways of DACs modulation by ipRGCs.



3.3 IpRGCs express synaptophysin in cultured retina

To ensure intra-retinal collaterals of ipRGCs are actually functional, we applied *ex vivo* electroporation technics to pup mice retinae. N1 vectors contained synaptophysin::eGFP sequence were sent into retinae extracted from P2 *Opn4^{cre/+}* mice. The retinae were observed after five day culture. Cells without activated *Opn4* promotor received vectors expressed dsRed while ipRGCs expressed synaptophysin::eGFP. (Figure 6A) Since synaptophysin participate presynaptic structure, conjugated eGFP would locate in functional presynapse as well. Conventional concept of retinal circuitry suppose that RGCs only innervate neuron in the brain via optic nerve. However we found eGFP express in IPL of cultured retina. (Figure 6B) Green fluorescence signals were arranged into axon-like form, indicating during developmental stage ipRGCs send feedback signals back to retina via intra-retinal axonal structure, which are quite likely to be collaterals of ipRGCs.



3.4 Ultrastructure of ipRGCs intra-retinal collaterals

To study furthermore detail and function of ipRGC intra-retinal axon terminal in adult mice, we tried to establish ultrastructure under transmission electron microscope. Retina samples were mounted into Spurr's resin after NBT/BCIP labeling (Figure 7A-B) of ipRGCs and optimized processing. A 0.99 μm semi-thin cross section (Figure 7C) was cut immediately after a series of 90 nm ultra-thin sections (Figure 7D), in order to compare brightfield semi-thin images and TEM ultra-thin images side by side.

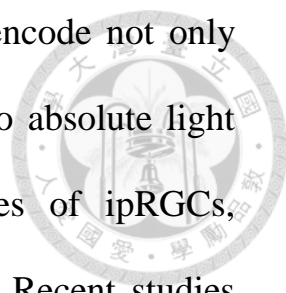
NBT/BCIP formed electron dense precipitations which appear in dark particles under TEM, made it possible to identify ipRGC collateral. Cell membrane as well as synaptic vesicles were enhanced by osmium tetroxide fixation and uranium acetate staining, appear in light gray in TEM images. Figure 7D showed an ipRGC collateral with NBT/BCIP particles and synaptic vesicles. There was corresponded postsynaptic density sitting opposite to synaptic vesicles, form complete synaptic structure. The synaptic structure indicates ipRGCs intra-retinal collaterals reach S1 sublayer of IPL are functional output routes for ipRGC sending feedback signals to retina.

Chapter 4. Discussion



The neural circuitry for vision perception and the subsequently light dark adaptation have been studied for more than a century.[3] Therefore, retina needs to actively adjust itself against an ambient light condition to optimize visual function, including coupling of multiple photoreceptor for dark adaptation, increasing bipolar gain for light adaptation and change the dopamine level to increase sensitivity. However, it is widely perceived that retinal ganglion cells, as the only output neuron in the retina, only transmit light information uni-directionally to thalamus in the brain without any kind of feedback circuit.

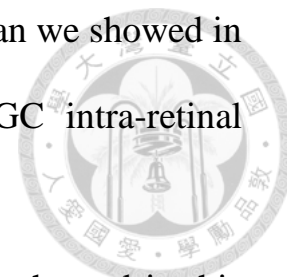
Intra-retinal axon collaterals of retinal ganglion cells were first reported thirty years ago. Existence of those collaterals suggests RGCs may modulate intra-retinal feedback regulations, which was conflicted to conventional viewpoint that RGCs transmit retinal output uni-directionally to brain. Therefore, functions or even existence of these collaterals were beyond debates for years. However, discovery of melanopsin expressing ipRGCs provides novel possibilities to retinal circuitry. Intrinsically photosensitive retinal ganglion cells generate different output when receiving light stimuli. Compared to conventional photoreceptor rod cells and cone cells, M1 ipRGC outputs to light are



slow-responded and sustained. Moreover, ipRGCs can encode not only light alteration like conventional photoreceptors, but also absolute light intensity information. Due to photosensitive properties of ipRGCs, information flow in retinal could be more complicated. Recent studies show ipRGCs may modulate retinal dopaminergic amacrine cells. Other studies show ipRGCs may also modulate retinal waves during developmental stages. All of these researches indicate ipRGCs participate intra-retinal feedback signaling.

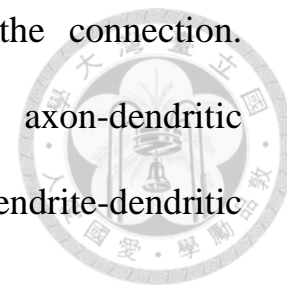
Previous study from our lab shows intra-retinal axon collaterals of ipRGCs by sparsely labelling. By furthermore research on morphology of ipRGCs, we show two distinct groups of the collaterals in this study. We also find synaptic structure on these collaterals under transmission electron microscope, indicating the collaterals are functional. However, in our sparsely labeling method, ipRGCs express higher level of melanopsin, which are M1 cells, are more likely to be labelled. Because of this reason, we are not able to observe all ipRGC intra-retinal collaterals. In fact, we have occasionally found M2 and M4 cells with collaterals. Another unpublished research shows functional intra-retinal axonal terminals of ipRGCs may distribute to entire retina using conditional expression of synaptophysin::GFP on ipRGCs. All of the above indicate that subtypes of ipRGCs with intra-retinal collaterals and

morphology of these collaterals may be more complex than we showed in this study. In the future, we would try to find ipRGC intra-retinal postsynaptic partners on GCaMP mice



Of two groups of ipRGC intra-retinal collaterals we showed in this study, we focused on collaterals co-stratified with dopaminergic amacrine cells in S1 sublayer of inner plexiform layer to find whether ipRGCs send feedback signals to DAC via the collaterals. The dopamine concentration in the retina is under control of the retinal circadian clock, independent of the mammalian central clock, suprachiasmatic nucleus, located in the hypothalamus.[28, 40] Recently studies show that dopamine regulates many retinal properties, including electroretinogram response, gap junction permeability between rod, cone and amacrine cells.[23-25] Since ipRGCs provide ambient light intensity information to SCN for circadian photoentrainment, they could also transmit local light intensity information to DACs by intra-retinal collaterals. Studies in our lab show that on rod and cone double-knocked mice, *c-fos* signals co-localize with DACs after illumination on retina roughly tile the retina. A recent study also displayed that 21% of DACs show sustained responses similar to M1 ipRGC output after light stimulation. Moreover, the responses are eliminated by applying tetrodotoxin.[21] These evidences show the connection from ipRGCs to DACs. By immunohistochemistry, here we

show intra-retinal collaterals of ipRGCs participate the connection. Result of tetrodotoxin application also supports axon-dendritic connections from ipRGCs to DACs other than dendrite-dendritic connections.



These feedback signals from ipRGCs could modify light detection gain at different retinal areas by altering dopamine level locally. The feedback signals may also modulate conventional photoreceptors by DAC neurite processes stratifying outer plexiform layer. Therefore, by modulating detection gain locally, our retina can process pattern information in parallel independent patches under uneven illumination across the entire visual field. Terminals of these axon collaterals in S1 sublayer may connect to both large-diameter, dendrite-liked neurites and small-diameter, axon-liked neurites of DACs. Dopaminergic amacrine cells have small “dendritic” fields and relatively larger “axonal” fields. Collaterals of ipRGCs connect to both neurites of DACs, suggesting ipRGCs may modulate retinal dopamine in different spatial levels. The two kinds of ipRGC-DAC synapses may be responsible for different ipRGC output intensity and involved into different adaptation circuits, which may be a possible explanation that retinal dopamine level is not changed in thousands of times as ambient illuminance changed dramatically. In the future, we can examine our ipRGC-modulated light

adaptation theory by performing electroretinogram on ipRGC-knocked out mice or retinal dopamine deficient mice.

Strikingly, some synaptic structures located on the ipRGC axon collaterals do not co-localized with DAC in our confocal images, which suggest that ipRGCs may provide ambient light information to other types of neurons retrogradely, possibly bipolar cells or other types of amacrine cells, to maintain fine light adaptation modulation.

Collaterals that do not reach S1 sublayer may have other functions. Previous studies show eliminating ipRGCs developmentally could alter retinal ganglion cell projection pattern in lateral geniculate nucleus.[29] Elimination of melanopsin also significantly decreases the firing frequency of spontaneous cholinergic retinal waves during the early postnatal stage.[29, 41] Cholinergic starburst amacrine cells (SACs) have dendrites stratifying in the S2 and the S4 sublayers in inner plexiform layer.[42, 43] Previous studies show early postnatal light experiment may have long-term effects on pattern vision performances.[44, 45] Another study also shows spontaneous neuronal activities may be modulated by ambient light.[46] If shallower collaterals connect to these SACs in developmental stage, it might explain the effect of ipRGC or melanopsin elimination on the normal retinal ganglion cell development. In our observation, shallower collaterals tend to be branchless single processes.

These single processes are possible to be dysfunction developmental traces and come from degeneration after developmental stages. During early postnatal days, the processes may be as complex as axons we showed in *ex vivo* electroporation result.

Through the advances of the research on ipRGCs, we discover that not only non-visual functions such as circadian photoentrainment are controlled by ipRGCs, but they also involve in the visual forming functions and even the development of visual circuitry between RGCs and LGN. Further study would give us a different view on this long-studied organ. Together, this study would open a new field of research on the retinal feedback circuitry, and advance our knowledge of retinal visual function through a population of specific neurons that is mainly involved in non-visual light functions.

4.1 Significance of the work

By using genetic sparsely labeling method, here we show there are at least two different morphologically distinct types of intra-retinal collateral from intrinsically photosensitive retinal ganglion cells (ipRGCs) that stratified retrograded at the inner plexiform layer. Furthermore, we demonstrated that collaterals co-stratified with dopaminergic amacrine cells (DACs) form putative synaptic contact with DACs by immunofluorescence and transmission electron microscopy. Together, these results indicate that ipRGCs send feedback signals to DACs, which are involved in many retinal functions including adaptation, circadian rhythm and contract sensitivity. We also found another population of ipRGC axon collaterals that stratified in the off-layer of the inner plexiform layer. These axon collateral may innervate other types of inter-neuron for different feedback functions. In addition, result of *ex vivo* electroporation indicates ipRGCs modulate retina by feedback signals via intra-retinal collaterals not only on adult but also during developmental stages. This study would open a new field of research on the retinal feedback circuitry, and advance our knowledge of retinal visual function through a population of specific neuron that is mainly involved in non-visual light functions.

Figures

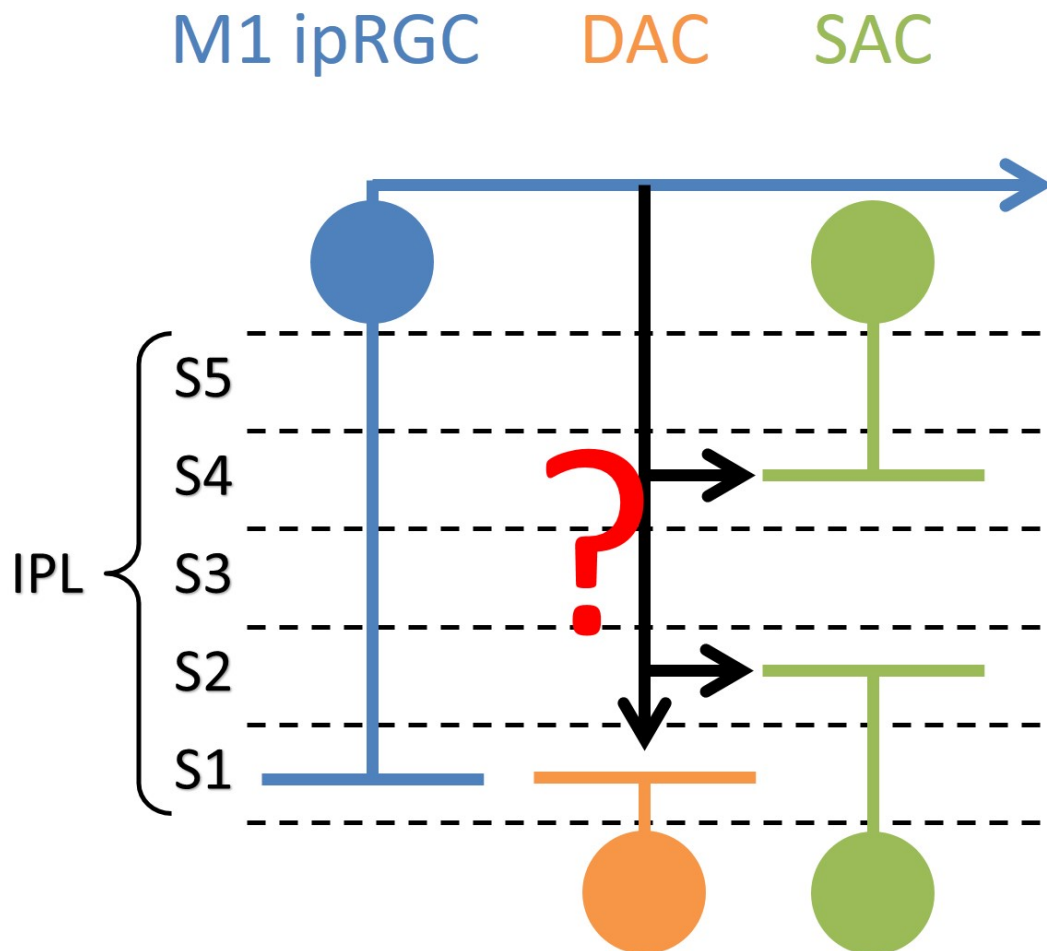


Figure 1. We hypothesized intrinsically photosensitive retinal ganglion cells (ipRGCs) send feedback signals to dopaminergic amacrine cells (DACs) by intra-retinal axon collateral co-stratified with DACs in S1 sublayer of inner plexiform layer (IPL).

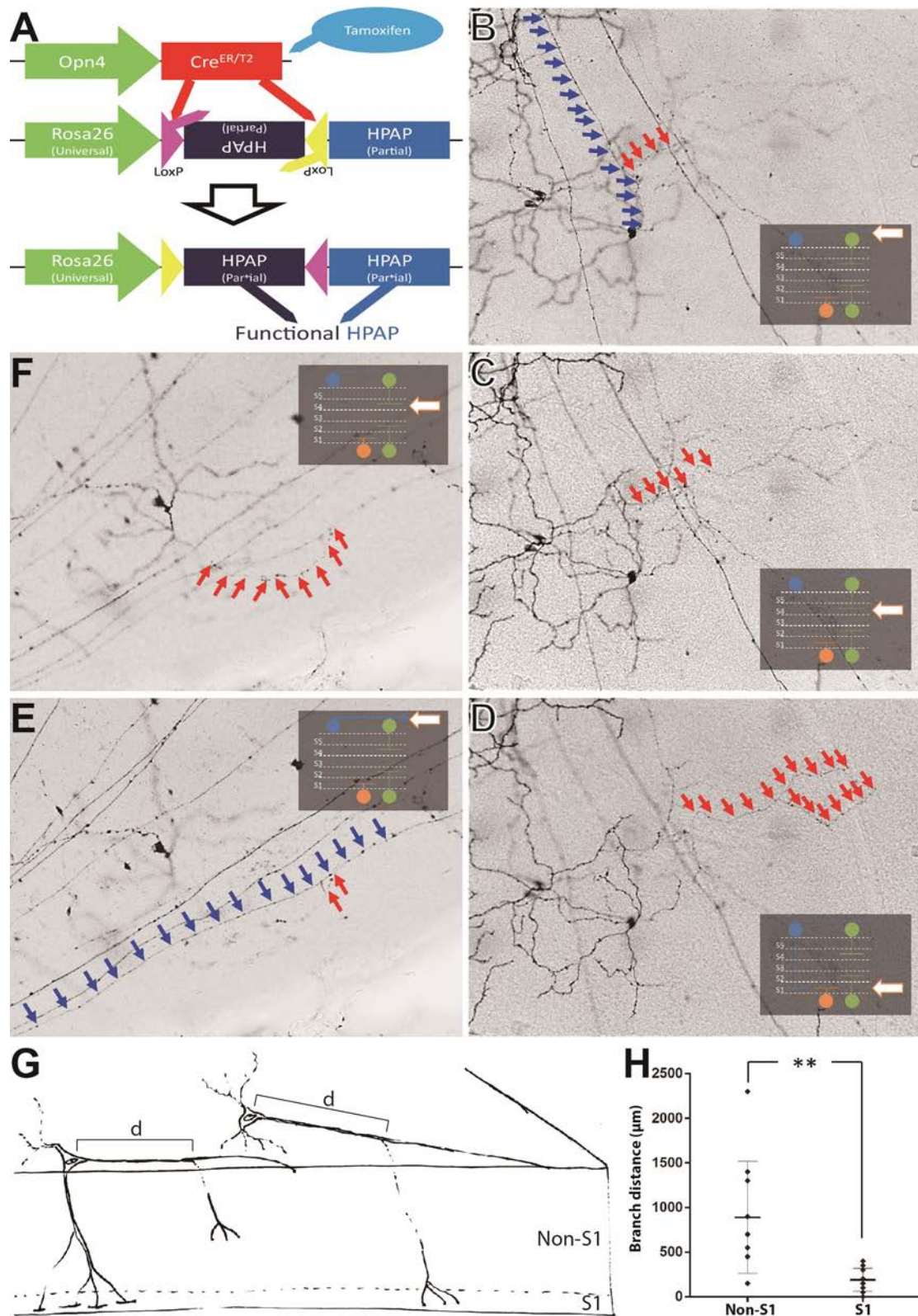


Figure 2. Morphological characteristics of intrinsically photosensitive retinal ganglion cells intra-retinal axon collaterals. **A.** An illustration of transgenic mice line for random ipRGCs labeling. Cre^{ER/T2} is driven by melanopsin promoter *Opn4*. Artificially applied tamoxifen is needed to conjugate with cre^{ER/T2} for operating endonucleus loxP sequence, activating functional human placental alkaline phosphatase (HPAP) driven by universal promoter *Rosa26*. Alkaline phosphatase produce dark-blueish precipitation with NBT/BCIP under histochemistry procedures. By adjusting tamoxifen dosage, number of ipRGCs presenting precipitation could be optimized to observe intra-retinal collaterals of ipRGCs. **B-F** demonstrated two dimensions of collaterals' characteristics. Firstly collaterals were different in complexity and can be classified into single collaterals (E-F) and complex collaterals (B-D). Secondly they were different in reached depth in inner plexiform layer (IPL). Some collaterals reached in deepest IPL and co-stratified with dopaminergic amacrine cells in S1 sub layer (B-D), while others did not reach that deep (E-F). Blue arrows indicate main axon of ipRGCs and red arrows indicate axon collaterals. Gray boxes indicate focal plans in IPL. Distance from soma to branch point was defined as "branch distance" and illustrated by "d" in **G**. **H** shows branch distances of collaterals reached S1 were significantly shorter than those collaterals don't reach

S1. (Student t test, $p=0.006$)



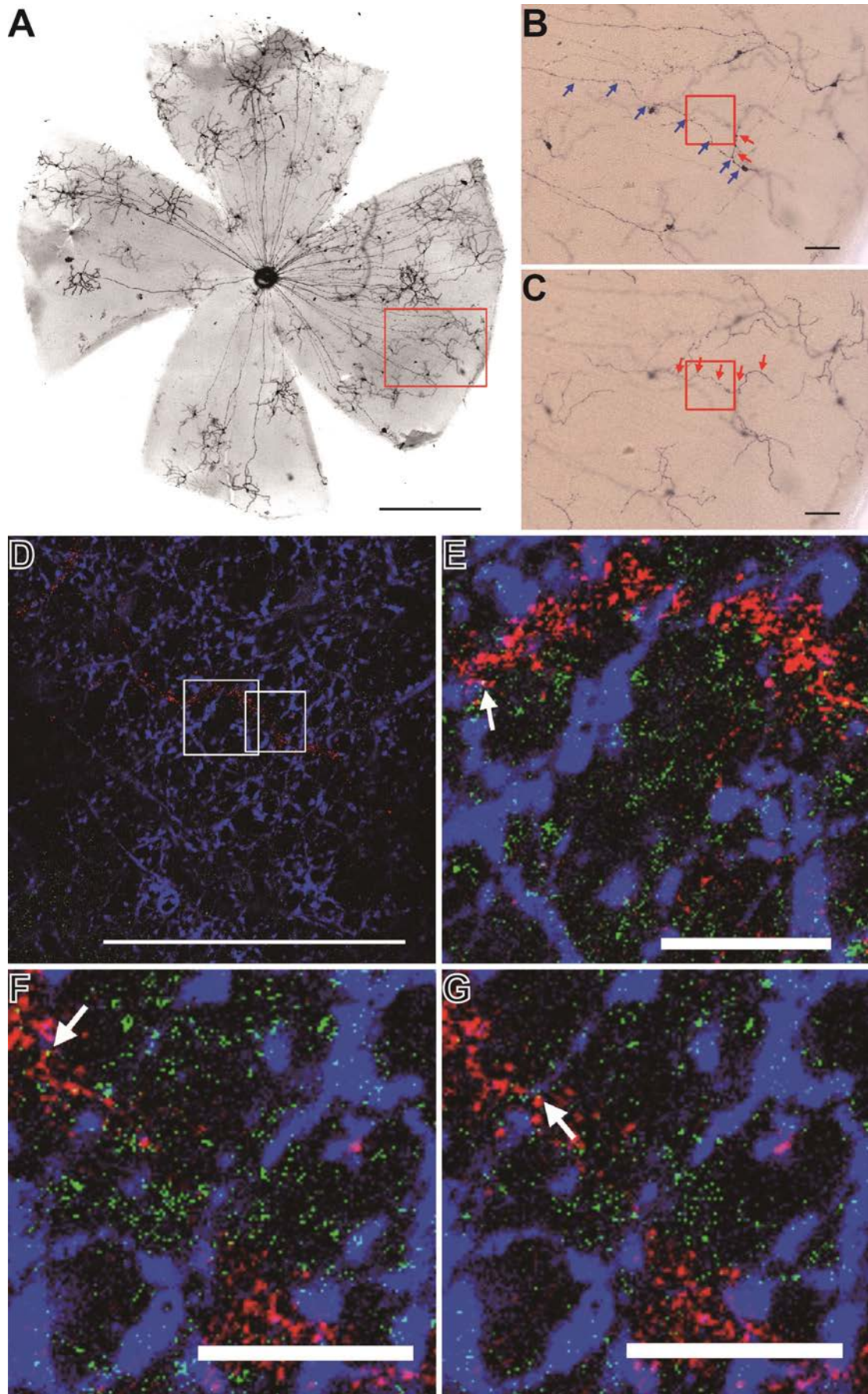


Figure 3. Collateral of ipRGCs contact with to dopaminergic amacrine cells. **A.** A whole-mounted retina with sparsely NBT/BCIP labeling. **B-C.** Higher magnifications in two focal plans of A showed an ipRGC with intra-retinal collateral. B and C were focus on ganglion cell layer and DAC stratified S1 sublayer, respectively. Blue arrows indicate main axon and red arrows indicate collateral. **D** shows confocal image of square region in C. **E-G.** Higher magnifications showed co-localization of ipRGC collateral (red), DACs (blue) and bassoon (green), indicated by white arrows. Scale bar: A 1 mm, B-D 100 μ m, E-G 10 μ m.

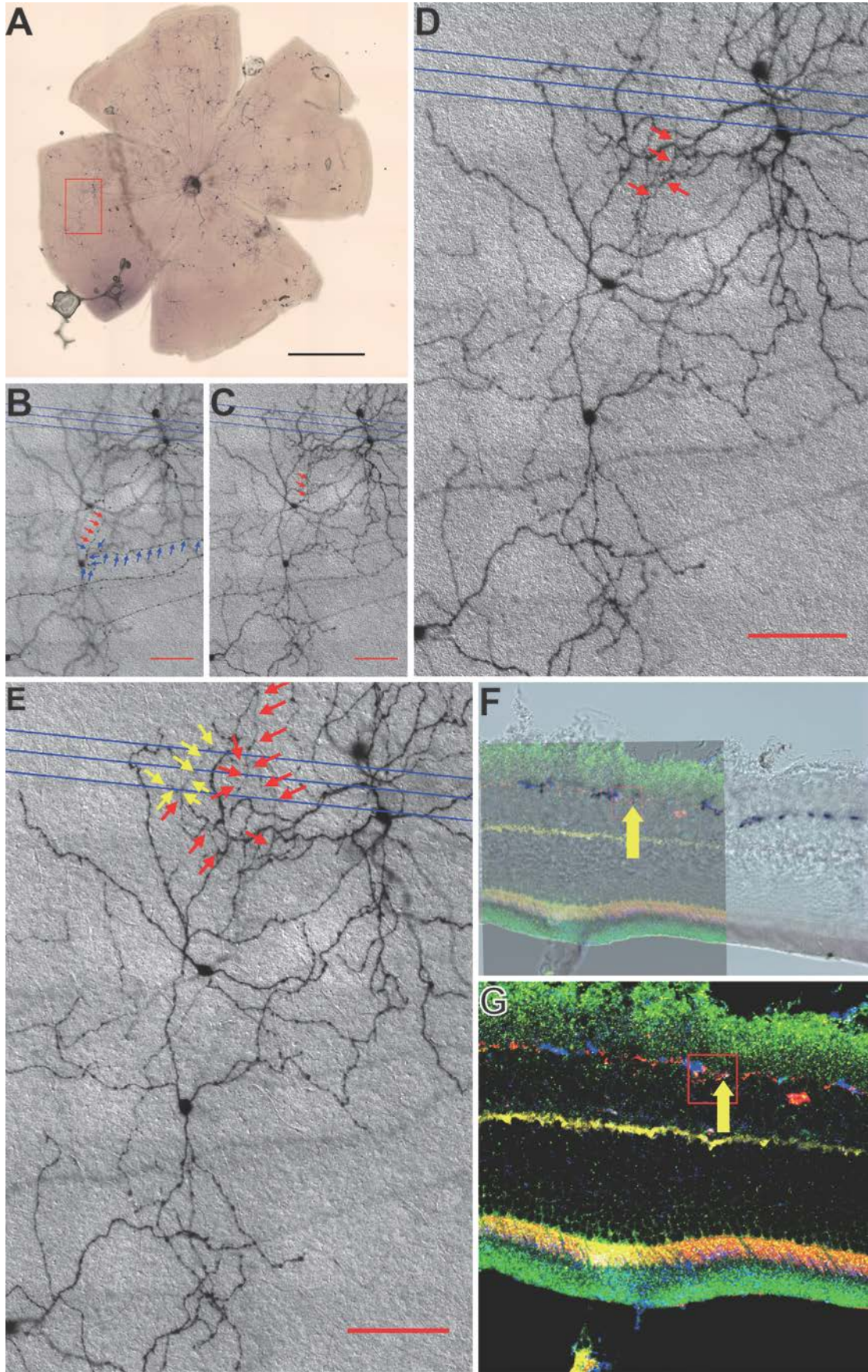


Figure 4. Cross section view of an ipRGC collateral. **A.** A whole-mounted retina with sparsely NBT/BCIP labeling. **B-E.** Higher magnifications of A under serial DIC images, focused from ganglion cell layer to boundary of inner plexiform layer and inner nucleus layer, respectively. Blue arrows indicate main axon and red arrows indicate collateral. Yellow arrows in E indicates collateral terminals in later figures. Two 20 μm cross sections were cut from A, location indicate by blue lines on B-E. Upper section is shown in **F.** Yellow arrow indicates same collateral terminal in E. **G.** Confocal image of F. Red, yellow, green and blue channels present immuno-positive of tyrosine hydroxylase, postsynaptic density, synaptophysin and NBT/BCIP precipitation in reflex mode, respectively. Yellow arrow indicates same collateral terminal in E. Scale bar: A 1 mm, B-E 100 μm .

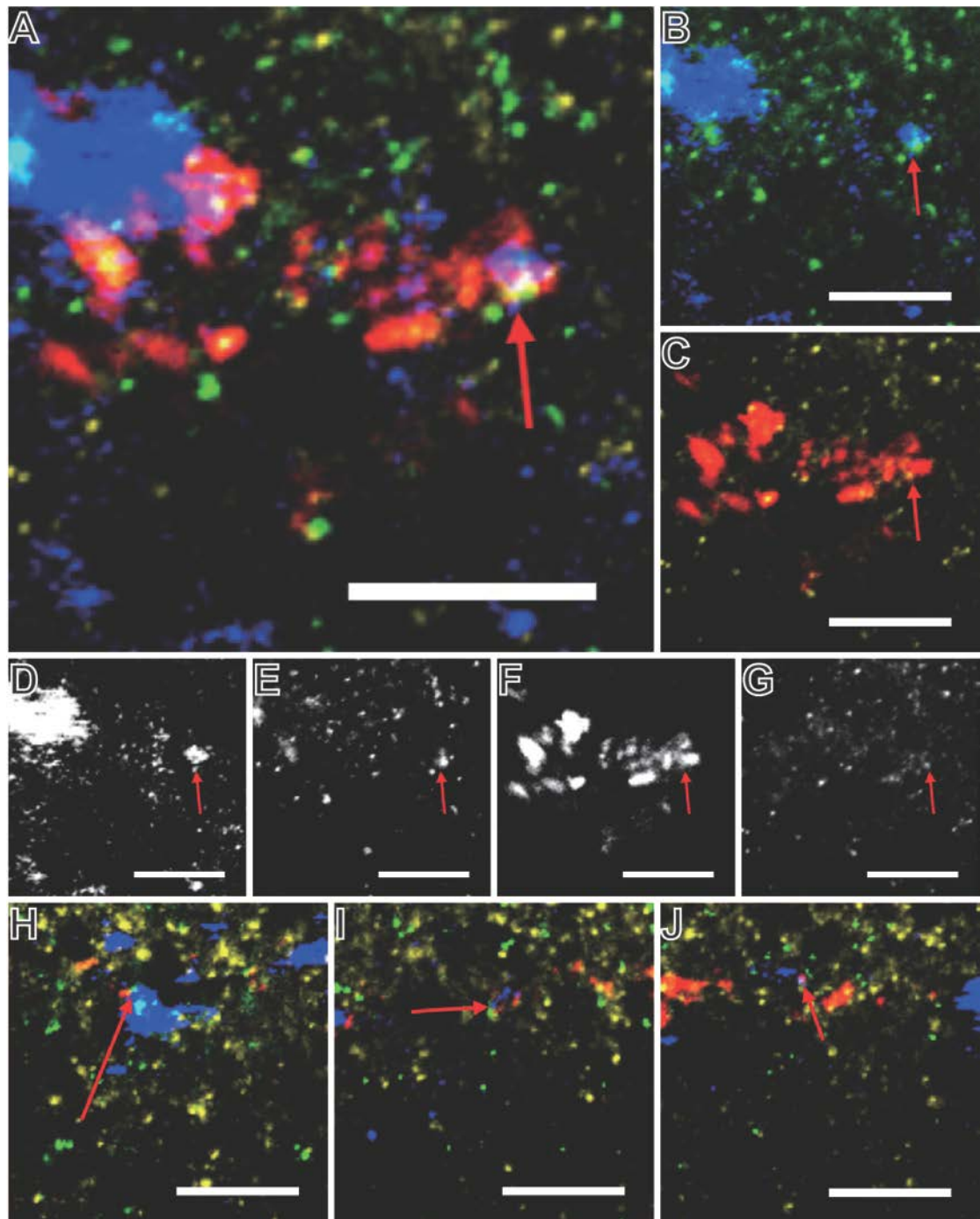
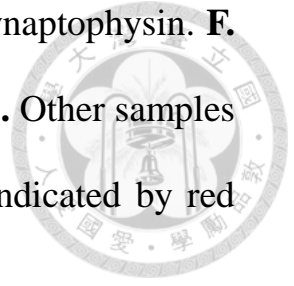


Figure 5. Collateral of ipRGC connect to DAC neurites. A. Higher magnification of figure 4G showed co-localization of ipRGC (blue) collateral, DAC (red), synaptophysin (SYP, green) and postsynaptic density (PSD, yellow), indicated by red arrow. **B-G.** Split channels of A.

B. IpRGC and SYP. **C.** DAC and PSD. **D.** IpRGC. **E.** Synaptophysin. **F.** Dopaminergic amacrine cell. **G.** Postsynaptic density. **H-J.** Other samples of co-localization in the other section from figure 4E, indicated by red arrows. Scale bar: 10 μ m.



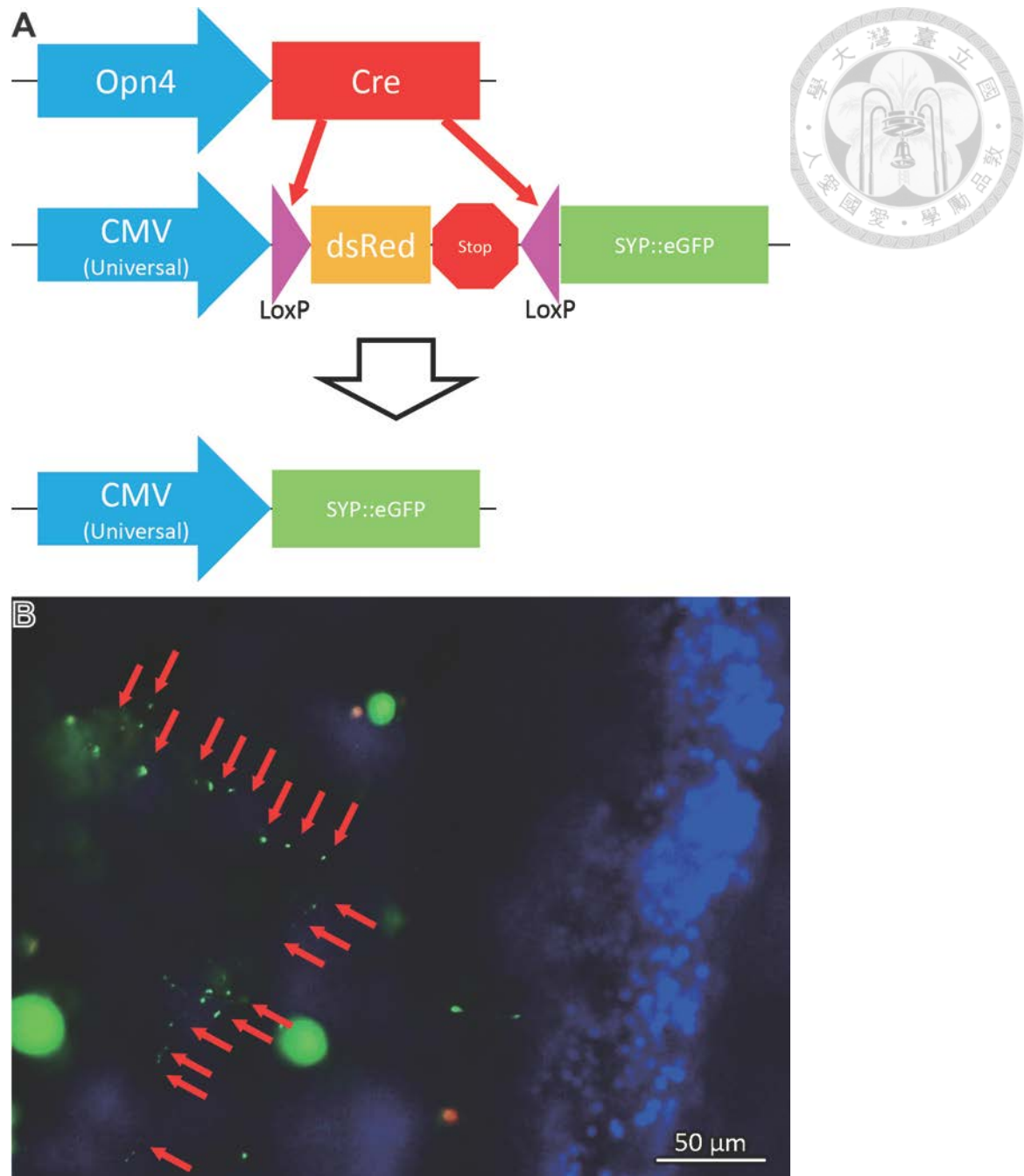


Figure 6. Melanopsin positive RGCs in cultured retina express synaptophysin. **A.** N1 vectors with synaptophysin::eGFP were sent into retina by *ex vivo* electroporation. Cells without activated *Opn4* promoter received vectors expressed dsRed, while ipRGCs expressed synaptophysin::eGFP. **B.** Retina from P2 mouse express eGFP after five

day culture, indicated by arrows.



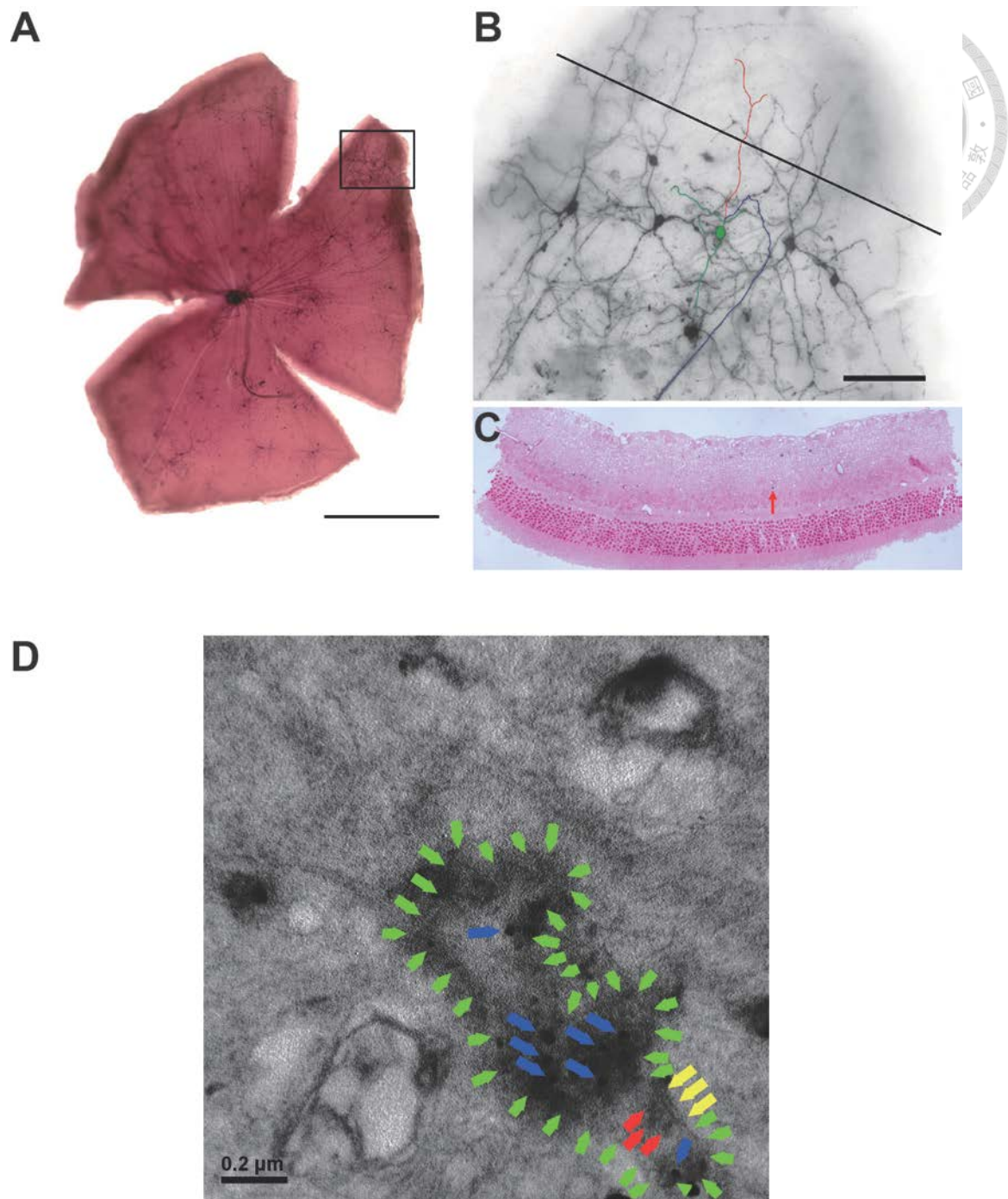


Figure 7. Synaptic ultra-structure of ipRGC collateral. **A.** A whole-mounted retina with sparsely NBT/BCIP labeling. **B.** Higher magnification of A. Green, blue and red indicate dendrites, main axon and axon collateral of an ipRGC, respectively. **C.** Cross section view of

bold line in B, counter stained with safranin O to indicate cell bodies. Red arrow indicates collateral. **D.** Synaptic ultra-structure of collateral under transmission electron microscope. NBT/BCIP formed electron dense precipitations appear in dark particles while cell membrane and synaptic vesicles were enhanced by osmium tetroxide fixation and uranium acetate staining, appear in light gray. Green, blue, red and yellow arrows indicate cell membrane of axon collateral, electron dense NBT/BCIP precipitation particles, synaptic vesicles and postsynaptic density. Scale bar: A 1 mm, B 100 μ m, D 200 nm.

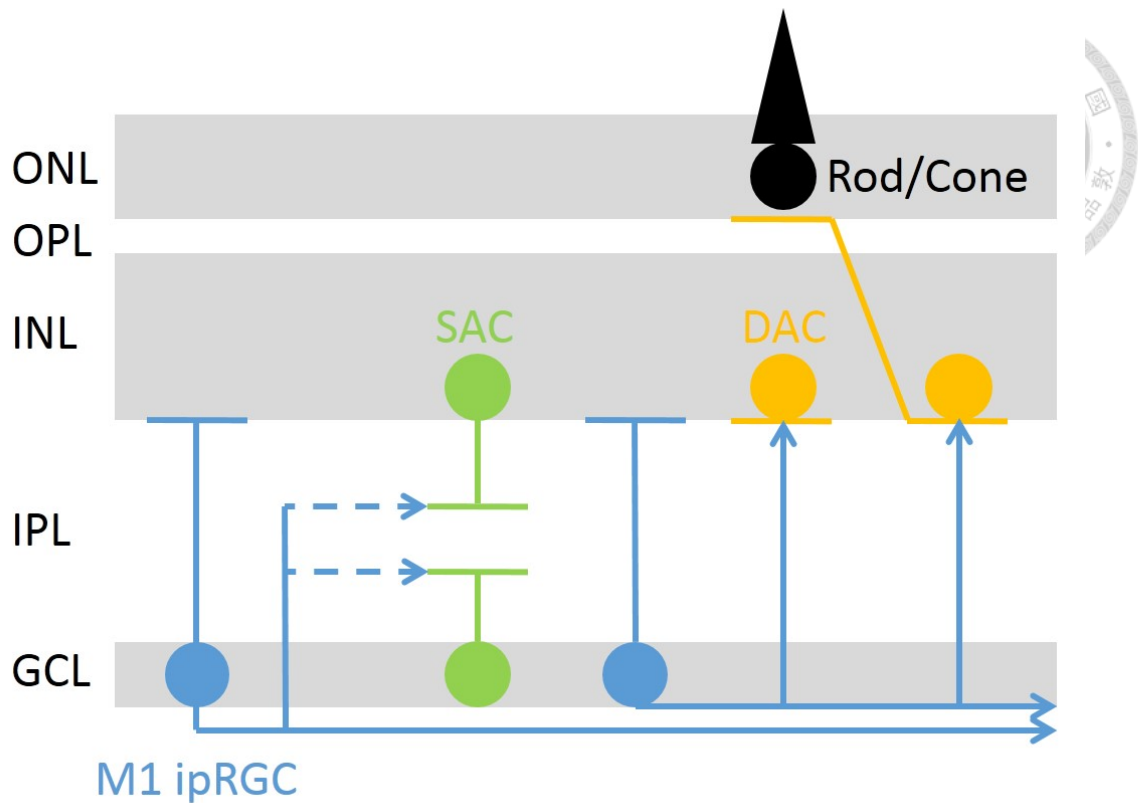
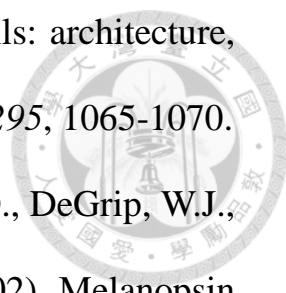


Figure 8. Illustration of the conclusion. We conclude our study that ipRGCs send feedback signals to DACs by intra-retinal collaterals co-stratified with DAC in S1 sublayer of inner plexiform layer, and furthermore modulate retinal circuitry by different DAC neurite. Collaterals don't co-stratified with DAC may also innervate to SACs during developmental stages and modulate retinal development.

References



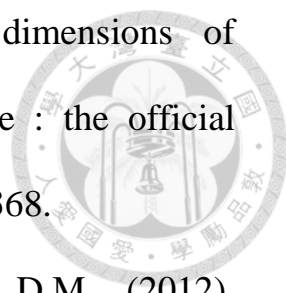
1. Wald, G. (1955). The photoreceptor process in vision. *American journal of ophthalmology* *40*, 18-41.
2. Wald, G. (1955). Visual pigments and vitamins A of the clawed toad, *Xenopus laevis*. *Nature* *175*, 390-391.
3. Wassle, H. (2004). Parallel processing in the mammalian retina. *Nature reviews. Neuroscience* *5*, 747-757.
4. Provencio, I., Rodriguez, I.R., Jiang, G., Hayes, W.P., Moreira, E.F., and Rollag, M.D. (2000). A novel human opsin in the inner retina. *The Journal of neuroscience : the official journal of the Society for Neuroscience* *20*, 600-605.
5. Provencio, I., Rollag, M.D., and Castrucci, A.M. (2002). Photoreceptive net in the mammalian retina. This mesh of cells may explain how some blind mice can still tell day from night. *Nature* *415*, 493.
6. Provencio, I., Jiang, G., De Grip, W.J., Hayes, W.P., and Rollag, M.D. (1998). Melanopsin: An opsin in melanophores, brain, and eye. *Proceedings of the National Academy of Sciences of the United States of America* *95*, 340-345.
7. Hattar, S., Liao, H.W., Takao, M., Berson, D.M., and Yau, K.W.

- 
- (2002). Melanopsin-containing retinal ganglion cells: architecture, projections, and intrinsic photosensitivity. *Science* 295, 1065-1070.
8. Panda, S., Sato, T.K., Castrucci, A.M., Rollag, M.D., DeGrip, W.J., Hogenesch, J.B., Provencio, I., and Kay, S.A. (2002). Melanopsin (Opn4) requirement for normal light-induced circadian phase shifting. *Science* 298, 2213-2216.
 9. Schmidt, T.M., Do, M.T., Dacey, D., Lucas, R., Hattar, S., and Matynia, A. (2011). Melanopsin-positive intrinsically photosensitive retinal ganglion cells: from form to function. *The Journal of neuroscience : the official journal of the Society for Neuroscience* 31, 16094-16101.
 10. Ecker, J.L., Dumitrescu, O.N., Wong, K.Y., Alam, N.M., Chen, S.K., LeGates, T., Renna, J.M., Prusky, G.T., Berson, D.M., and Hattar, S. (2010). Melanopsin-expressing retinal ganglion-cell photoreceptors: cellular diversity and role in pattern vision. *Neuron* 67, 49-60.
 11. Schmidt, T.M., Alam, N.M., Chen, S., Kofuji, P., Li, W., Prusky, G.T., and Hattar, S. (2014). A role for melanopsin in alpha retinal ganglion cells and contrast detection. *Neuron* 82, 781-788.
 12. Panda, S., Provencio, I., Tu, D.C., Pires, S.S., Rollag, M.D., Castrucci, A.M., Pletcher, M.T., Sato, T.K., Wiltshire, T., Andahazy,

- M., et al. (2003). Melanopsin is required for non-image-forming photic responses in blind mice. *Science* 301, 525-527.
13. Takahashi, J.S., DeCoursey, P.J., Bauman, L., and Menaker, M. (1984). Spectral sensitivity of a novel photoreceptive system mediating entrainment of mammalian circadian rhythms. *Nature* 308, 186-188.
14. Freedman, M.S., Lucas, R.J., Soni, B., von Schantz, M., Munoz, M., David-Gray, Z., and Foster, R. (1999). Regulation of mammalian circadian behavior by non-rod, non-cone, ocular photoreceptors. *Science* 284, 502-504.
15. Rollag, M.D., Berson, D.M., and Provencio, I. (2003). Melanopsin, ganglion-cell photoreceptors, and mammalian photoentrainment. *Journal of biological rhythms* 18, 227-234.
16. Lucas, R.J., Hattar, S., Takao, M., Berson, D.M., Foster, R.G., and Yau, K.W. (2003). Diminished pupillary light reflex at high irradiances in melanopsin-knockout mice. *Science* 299, 245-247.
17. Xue, T., Do, M.T., Riccio, A., Jiang, Z., Hsieh, J., Wang, H.C., Merbs, S.L., Welsbie, D.S., Yoshioka, T., Weissgerber, P., et al. (2011). Melanopsin signalling in mammalian iris and retina. *Nature* 479, 67-73.
18. Chen, S.K., Badea, T.C., and Hattar, S. (2011). Photoentrainment

and pupillary light reflex are mediated by distinct populations of ipRGCs. *Nature* 476, 92-95.

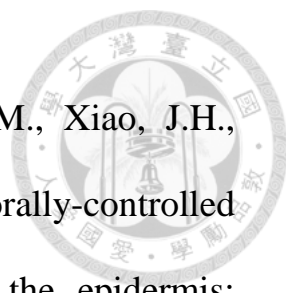
19. Semo, M., Gias, C., Ahmado, A., and Vugler, A. (2014). A role for the ciliary marginal zone in the melanopsin-dependent intrinsic pupillary light reflex. *Experimental eye research* 119, 8-18.
20. Dacey, D.M. (1990). The dopaminergic amacrine cell. *The Journal of comparative neurology* 301, 461-489.
21. Zhang, D.Q., Wong, K.Y., Sollars, P.J., Berson, D.M., Pickard, G.E., and McMahon, D.G. (2008). Intraretinal signaling by ganglion cell photoreceptors to dopaminergic amacrine neurons. *Proceedings of the National Academy of Sciences of the United States of America* 105, 14181-14186.
22. Zhang, D.Q., Belenky, M.A., Sollars, P.J., Pickard, G.E., and McMahon, D.G. (2012). Melanopsin mediates retrograde visual signaling in the retina. *PloS one* 7, e42647.
23. Hampson, E.C., Vaney, D.I., and Weiler, R. (1992). Dopaminergic modulation of gap junction permeability between amacrine cells in mammalian retina. *The Journal of neuroscience : the official journal of the Society for Neuroscience* 12, 4911-4922.
24. Jackson, C.R., Ruan, G.X., Aseem, F., Abey, J., Gamble, K., Stanwood, G., Palmiter, R.D., Iuvone, P.M., and McMahon, D.G.

- 
- (2012). Retinal dopamine mediates multiple dimensions of light-adapted vision. *The Journal of neuroscience : the official journal of the Society for Neuroscience* 32, 9359-9368.
25. Van Hook, M.J., Wong, K.Y., and Berson, D.M. (2012). Dopaminergic modulation of ganglion-cell photoreceptors in rat. *The European journal of neuroscience* 35, 507-518.
26. Dkhissi-Benyahya, O., Coutanson, C., Knoblauch, K., Lahouaoui, H., Leviel, V., Rey, C., Bennis, M., and Cooper, H.M. (2013). The absence of melanopsin alters retinal clock function and dopamine regulation by light. *Cellular and molecular life sciences : CMLS* 70, 3435-3447.
27. Dubocovich, M.L., Lucas, R.C., and Takahashi, J.S. (1985). Light-dependent regulation of dopamine receptors in mammalian retina. *Brain research* 335, 321-325.
28. He, Q., Xu, H.P., Wang, P., and Tian, N. (2013). Dopamine D1 receptors regulate the light dependent development of retinal synaptic responses. *PloS one* 8, e79625.
29. Renna, J.M., Weng, S., and Berson, D.M. (2011). Light acts through melanopsin to alter retinal waves and segregation of retinogeniculate afferents. *Nature neuroscience* 14, 827-829.
30. Peterson, B.B., and Dacey, D.M. (1998). Morphology of human

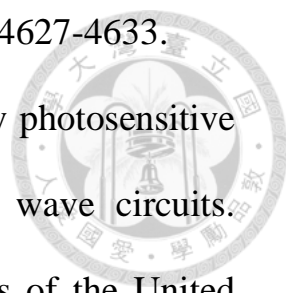
retinal ganglion cells with intraretinal axon collaterals. *Visual neuroscience* 15, 377-387.

31. Dacey, D.M. (1989). Axon-bearing amacrine cells of the macaque monkey retina. *The Journal of comparative neurology* 284, 275-293.
32. Dacey, D.M. (1985). Wide-spreading terminal axons in the inner plexiform layer of the cat's retina: evidence for intrinsic axon collaterals of ganglion cells. *The Journal of comparative neurology* 242, 247-262.
33. Joo, H.R., Peterson, B.B., Dacey, D.M., Hattar, S., and Chen, S.K. (2013). Recurrent axon collaterals of intrinsically photosensitive retinal ganglion cells. *Visual neuroscience* 30, 175-182.
34. Metzger, D., Clifford, J., Chiba, H., and Chambon, P. (1995). Conditional site-specific recombination in mammalian cells using a ligand-dependent chimeric Cre recombinase. *Proceedings of the National Academy of Sciences of the United States of America* 92, 6991-6995.
35. Kam, W., Clauser, E., Kim, Y.S., Kan, Y.W., and Rutter, W.J. (1985). Cloning, sequencing, and chromosomal localization of human term placental alkaline phosphatase cDNA. *Proceedings of the National Academy of Sciences of the United States of America*

82, 8715-8719.

- 
36. Indra, A.K., Warot, X., Brocard, J., Bornert, J.M., Xiao, J.H., Chambon, P., and Metzger, D. (1999). Temporally-controlled site-specific mutagenesis in the basal layer of the epidermis: comparison of the recombinase activity of the tamoxifen-inducible Cre-ER(T) and Cre-ER(T2) recombinases. *Nucleic acids research* 27, 4324-4327.
37. Snyder, E.Y., Deitcher, D.L., Walsh, C., Arnold-Aldea, S., Hartwig, E.A., and Cepko, C.L. (1992). Multipotent neural cell lines can engraft and participate in development of mouse cerebellum. *Cell* 68, 33-51.
38. Spurr, A.R. (1969). A low-viscosity epoxy resin embedding medium for electron microscopy. *Journal of ultrastructure research* 26, 31-43.
39. Wang, Q., Li, A., Gong, H., Xu, D., and Luo, Q. (2012). Quantitative study on the hygroscopic expansion of spurr resin to obtain a high-resolution atlas of the mouse brain. *Experimental biology and medicine* 237, 1134-1141.
40. Jackson, C.R., Capozzi, M., Dai, H., and McMahon, D.G. (2014). Circadian perinatal photoperiod has enduring effects on retinal dopamine and visual function. *The Journal of neuroscience : the*

official journal of the Society for Neuroscience 34, 4627-4633.

- 
41. Kirkby, L.A., and Feller, M.B. (2013). Intrinsically photosensitive ganglion cells contribute to plasticity in retinal wave circuits. *Proceedings of the National Academy of Sciences of the United States of America* 110, 12090-12095.
42. Famiglietti, E.V., Jr. (1983). 'Starburst' amacrine cells and cholinergic neurons: mirror-symmetric on and off amacrine cells of rabbit retina. *Brain research* 261, 138-144.
43. Koontz, M.A., and Hendrickson, A.E. (1987). Stratified distribution of synapses in the inner plexiform layer of primate retina. *The Journal of comparative neurology* 263, 581-592.
44. Wong, R.O. (1999). Retinal waves: stirring up a storm. *Neuron* 24, 493-495.
45. Wong, R.O. (1999). Retinal waves and visual system development. *Annual review of neuroscience* 22, 29-47.
46. Friedmann, D., Hoagland, A., Berlin, S., and Isacoff, E.Y. (2015). A spinal opsin controls early neural activity and drives a behavioral light response. *Current biology : CB* 25, 69-74.

Appendix



Buffers and formulas

Phosphate buffer saline (PBS)

Mix 0.1M sodium phosphate monobasic and 0.1M sodium phosphate dibasic in 40.5:9.5 ratio and solve 0.9% sodium chloride in the solution.

Adjust to pH 7.4 (or pH 6.8 in 10x prepare) by NaOH or HCl.

Dissecting buffer

10X HBSS	200ml	GIBCO #14065-056
1M HEPES	20ml	Sigma #H7523
+ NaHCO ₃	0.7g	

Add the water till 1800ml in 2L bottle.

Adjust solution to pH 7.35 by NaOH. Solution should be filtered and then store in 4 °C.

Culture buffer

Item and concentration	For 10ml	Cat. No.
Neural Basal A medium	9.6ml	GIBCO #10888
Glucose (0.6%)	0.06	

L-Glutamine (200mM Stock)	100ul	Sigma #G-6392
B27 Supplement (50X stock)	200ul	GIBCO #17504-044
HEPES (1M, pH 7.35-7.4)	100ul	
Sodium pyruvate (100mM Stock)	100ul	GIBCO #11360-070
Insulin (200X; 0.5mg/ml Stock, pH 2.5 in H2O)	50ul	Sigma #I1882
Penicillin/Streptomycin (10mg/ml)	100ul	GIBCO #15140
Forskolin (30 mM stock)	2ul	Sigma #F-6886

Forskolin should be applied after filtering the solution.

Cacodylate buffer with sucrose (CBC)

0.1M sodium cacodylate, 4% sucrose, 0.05M MgCl₂ and 0.05M CaCl₂,
pH 7.4 (adjusted by HCl)

Spurr's resin A

It would be better to prepare Spurr's resin in dry days (RH < 50%). We used EMS "low viscosity embedding media Spurr's kit" (cat. #14300) here. The mixture can be stored in 4 °C for a week. and should be warmed up by room temperature for 20-30 min before use. Although mixture can be store in sealed container in -20 °C for 1-2 months, fresh

prepared resin is always recommended. Optimized formulas for retina are listed below.



ERL 4221 5.00g

DER 736 3.80g

NSA 13.0g

Spurr's resin B

ERL 4221 5.00g

DER 736 3.80g

NSA 13.0g

This three compound should be mixed thoroughly before adding DAME.

DAME 0.15g

Antibodies

Primary antibodies

Antigen	Host	Dose	Brand
Bassoon	Mouse IgG2a	1/400	Enzo
PSD95	Rabbit	1/200	Abcam
Synaptophysin (SYP)	Chicken	1/1000	Abcam
Tyrosine hydroxylase (TH)	Mouse IgG1	1/1000	ImmunoStar

Secondary antibodies

Antigen	Host	Primary antibody	Fluorophore	Dose	Brand
Chicken	Goat	SYP	Alexa 488	1/500	Biotium
Mouse IgG1	Goat	TH	Alexa 568	1/500	Biotium
Mouse IgG1	Goat	TH	Alexa 594	1/500	Invitrogen
Mouse IgG2a	Goat	Bassoon	Alexa 488	1/500	Biotium
Rabbit	Goat	PSD95	Alexa 568	1/500	Biotium

Synaptophysin::eGFP vector sequence

Insert following sequence into N1 vector by *XhoI* and *NotI*.

CTCGAGATAACTTCGTATAGCATAACATTATACGAAGTTAT(*LoxP*)A
 AGCTTGCCACCATGCTGTGCTGCATCAGAAGAACTAAACCGGT
 TGAGAAGAATGAAGAGGCCGATCAGGAGCTGTCTAGAATGGCC
 TCCTCCGAGAACGTCATCACCGAGTTCATGCGCTTCAAGGTGC
 GCATGGAGGGCACCGTGAACGGCCACGAGTTCGAGATCGAGG
 GCGAGGGCGAGGGCCGCCCTACGAGGGCCACAACACCGTGA
 AGCTGAAGGTGACCAAGGGCGGCCCTGCCCTTCGCCTGGGA
 CATCTGTCCCCCAGTTCAGTACGGCTCCAAGGTGTACGTGA
 AGCACCCCGCCGACATCCCCGACTACAAGAAGCTGTCCTTCCC
 CGAGGGCTTCAAGTGGGAGCGCGTGATGAACTTCGAGGACGG

CGGCGTGGCGACCGTGACCCAGGACTCCTCCCTGCAGGACGGC
TGCTTCATCTACAAGGTGAAGTTCATCGGCGTGAACCTCCCTC
CGACGGCCCCGTGATGCAGAAGAAGACCATGGGCTGGGAGGC
CTCCACCGAGCGCCTGTACCCCCGCGACGGCGTGCTGAAGGGC
GAGACCCACAAGGCCCTGAAGCTGAAGGACGGCGGCCACTAC
CTGGTGGAGTTCAAGTCCATCTACATGGCCAAGAAGCCCGTGC
AGCTGCCCGGCTACTACTACGTGGACGCCAAGCTGGACATCAC
CTCCACAACGAGGACTACACCATCGTGGAGCAGTACGAGCGC
ACCGAGGGCCGCCACCACCTGTTCTGTAG(*dsRed*)CTAGCTAGG
GTACCGGGCCCCCCTCGAGATAACTTCGTATAGCATAATTATA
CGAAGTTAT(*LoxP*)AAGCTTATGGACGTGGTGAATCAGCTGGTG
GCTGGGGGTCAGTTCCGGGTGGTCAAGGAGCCCCTTGGCTTTG
TGAAGGTGCTGCAGTGGGTCTTTGCCATCTTCGCCTTTGCTACG
TGTGGCAGCTACACCGGGGAGCTTCGGCTGAGCGTGGAGTGTG
CCAACAAGACGGAGAGTGCCCTCAACATCGAAGTTGAATTCGA
GTACCCCTTCAGGCTGCACCAAGTGTACTTTGATGCACCCTCCT
GCGTCAAAGGGGGCACTACCAAGATCTTCCTGGTTGGGGACTA
CTCCTCGTCGGCTGAATTCTTTGTACCGTGGCTGTGTTTGCCT
TCCTCTACTCCATGGGGGCCCTGGCCACCTACATCTTCCTGCAG
AACAAGTACCGAGAGAACAACAAGGGCCTATGATGGACTTTC
TGGCTACAGCCGTGTTTCGCTTTCATGTGGCTAGTTAGTTCATCA

GCCTGGGCCAAAGGCCTGTCCGATGTGAAGATGGCCACGGACC
CAGAGAACATTATCAAGGAGATGCCCATGTGCCGCCAGACAGG
GAACACATGCAAGGAACTGAGGGACCCTGTGACTTCAGGACTC
AACACCTCAGTGGTGTGGCTTCCTGAACCTGGTGCTCTGGG
TTGGCAACTTATGGTTCGTGTTCAAGGAGACAGGCTGGGCAGC
CCCATTCATGCGCGCACCTCCAGGCGCCCCGAAAAGCAACCA
GCACCTGGCGATGCCTACGGCGATGCGGGCTACGGGCAGGGCC
CCGGAGGCTATGGGCCCCAGGACTCCTACGGGCCTCAGGGTGG
TTATCAACCCGATTACGGGCAGCCAGCCAGCGGTGGCGGTGGC
TACGGGCCTCAGGGCGACTATGGGCAGCAAGGCTATGGCCAAC
AGGGTGCGCCCACCTCCTTCTCCAATCAGATGCCGCGG(*Synapto*
-physin)GCCCGGGATCCACCGGTGCGCCACCATGGTGAGCAAGGG
CGAGGAGCTGTTCACCGGGGTGGTGCCCATCCTGGTCGAGCTG
GACGGCGACGTAAACGGCCACAAGTTCAGCGTGTCCGGCGAG
GGCGAGGGCGATGCCACCTACGGCAAGCTGACCCTGAAGTTCA
TCTGCACCACCGGCAAGCTGCCCGTGCCCTGGCCCACCCTCGT
GACCACCCTGACCTACGGCGTGCAGTGCTTCAGCCGCTACCCC
GACCACATGAAGCAGCACGACTTCTTCAAGTCCGCCATGCCCG
AAGGCTACGTCCAGGAGCGCACCATCTTCTTCAAGGACGACGG
CAACTACAAGACCCGCGCCGAGGTGAAGTTCGAGGGCGACAC
CCTGGTGAACCGCATCGAGCTGAAGGGCATCGACTTCAAGGAG

GACGGCAACATCCTGGGGCACAAGCTGGAGTACAACTACAACA
GCCACAACGTCTATATCATGGCCGACAAGCAGAAGAACGGCAT
CAAGGTGAACTTCAAGATCCGCCACAACATCGAGGACGGCAGC
GTGCAGCTCGCCGACCACTACCAGCAGAACACCCCCATCGGGC
ACGGCCCCGTGCTGCTGCCCGACAACCACTACCTGAGCACCCA
GTCCGCCCTGAGCAAAGACCCCAACGAGAAGCGCGATCACATG
GTCCTGCTGGAGTTCGTGACCGCCGCGGGATCACTCTCGGCA
TGGACGAGCTGTACAAG(*eGFP*)TAAAGCGGCCGC

Chemicals and commercial reagent

Calcium chloride (anhydrous): J.T.Baker 1311-01 Lot#0000024781

Lead citrate: Electron Microscopy Science #17800 Lot#890322

Magnesium chloride: Sigma M8266 Lot#11M0118V

NBT/BCIT (tablet) Roche 11697471001 Lot#10559000

OCT compound: Sakura 4583 Lot#0004348-01

Paraformaldehyde Sigma-Aldrich 158127 Lot#BCBJ1144V

Sodium cacodylate (trihydrate): Electron Microscopy Science #124-65-2
Lot#030130

Sodium Chloride (crystal): J.T.Baker 3624-05 Lot#0000006228

Sodium phosphate, dibasic (anhydrous): J.T.Baker 3829-69 Lot#K20142

Sodium phosphate, monobasic (monohydrate, crystal): J.T.Baker 3818-69

Lot#G22149

Sucrose (crystal): J.T.Baker 4072-05 Batch#0000024483

Sunflower seed oil: Sigma S5007 Lot#MKBK1503V

Triton X-100: Sigma X-100 Lot#BB1491V

Trizma base: Sigma T1503 Lot#SLBC4082V

Vectashield with DAPI: Vector Laboratories H-1200



Devices

Microtome: Leica cryostat microtome and Ultracut E.

Brightfield and fluorescent microscope: Zeiss Observer Z.1 with Zeiss MRc camera. Operating by software ZEN 2012.

Confocal microscope: Zeiss LSM 780 system, operating by software ZEN 2010.

Transmission electron microscope: Hitachi H-7650 with Gatan ES500 camera.